Vortex Lattice Structures of a Bose-Einstein Condensate in a Rotating Lattice Potential

Toshihiro Sato*, Tomohiko Ishiyama and Tetsuro Nikuni

*The Institute for Solid State Physics, The University of Tokyo, 5-1-5 Kashiwanoha, Kashiwa, Chiba 277-8581, Japan**
Tokyo University of Science, 1-3 Kagurazaka, Shinjuku-ku, Tokyo, 162-9601, Japan

We study vortex lattice structures of a trapped Bose-Einstein condensate in a rotating lattice potential by numerically solving the time-dependent Gross-Pitaevskii equation. By rotating the lattice potential, we observe the transition from the Abrikosov vortex lattice to the pinned lattice. We investigate the transition of the vortex lattice structure by changing conditions such as angular velocity, intensity, and lattice constant of the rotating lattice potential.

PACS numbers: 03.75.Lm, 03.75.Kk

Quantized vortices are one of the most characteristic manifestations of superfluidity associated with a Bose-Einstein condensate (BEC) in atomic gases. By rotating anisotropic trap potentials, several experimental groups observed formation of triangular Abrikosov lattices of vortices in rotating BECs [1,2,3]. Microscopic mechanism of the vortex lattice formation has been extensively studied both analytically and numerically using the Gross-Pitaevskii (GP) equation for the condensate wavefunction [4,5,6,7,8,9,10,11]. More recently, the vortex phase diagrams of a BEC in rotating lattice potentials have attracted theoretical attention, since one expects vortex pinning and structural phase transition of vortex lattice structures [12,13,14]. Recently, a rotating lattice has been experimentally realized at JILA, makinig use of a laser beam passing through a rotating mask [12]. Stimulated by the recent JILA experiment, in this paper, we study vortex lattice structures of a BEC in a rotating triangular lattice potential created by blue-detuned laser beams.

We numerically solve the two-dimensional Gross-Pitaevskii (GP) equa-

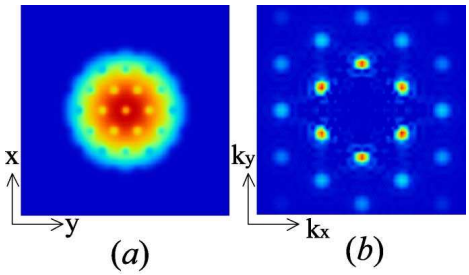

Fig. 1. Density profile (a) and Structure factor profile (b) of BEC in the lattice potential. The lattice potential geometry is triangular lattice at $a/a_{ho} = 2.2$ and $\sigma/a_{ho} = 0.65$.

tion in a frame rotationg with anguler velocity Ω:

$$(i-\gamma)\hbar\frac{\partial\psi(\mathbf{r},t)}{\partial t} = \left[-\frac{\hbar^2}{2m}\nabla^2 + V_{\rm ext}(\mathbf{r}) + g|\psi(\mathbf{r},t)|^2 - \Omega L_z\right]\psi(\mathbf{r},t). \qquad (1)$$

Here the total external potential is given by $V_{\rm ext}(\mathbf{r}) = m\omega_0(x^2+y^2)/2 + V_{\rm lattice}(\mathbf{r})$, $L_z = -i\hbar(x\frac{\partial}{\partial y} - y\frac{\partial}{\partial x})$ is the z component of the anguler momenum operator, $g = 4\pi\hbar^2 a_s/m$ is the strength of interaction with a_s being the s-wave scattering length, and γ is the phenomenolocical dissipative parameter [15,16,17,18,19]. The lattice potential created by blue-detuned laser beams arranged in the lattice geometry is expressed as

$$V_{\rm lattice}(\mathbf{r}) = \sum_{n_1,n_2} V_0 \exp\left[-\frac{|\mathbf{r}-\mathbf{r}_{n_1,n_2}|^2}{(\sigma/2)^2}\right], \qquad (2)$$

where $\mathbf{r}_{n_1,n_2} = n_1\mathbf{a}_1 + n_2\mathbf{a}_2$. We consider the triangular lattice geometry with the lattice constant a: $\mathbf{a}_1 = a(1,0)$, $\mathbf{a}_2 = a(-1/2, \sqrt{3}/2)$. Throughout this paper, we scale the length and energy by $a_{ho} = \sqrt{\hbar/m\omega_0}$ and $\hbar\omega_0$. We set the dimentionless interaction strength as $C = 4\pi a_s N/h_z = 1000$, where N is the total particle number and h_z is a height of the cylinder, and the width of the laser beam as $\sigma/a_{ho} = 0.65$. In our parameter set, the healing length is $\xi/a_{ho} = 0.12$.

In our simulations, we first determine the ground-state condensate wavefunction without rotation by setting $\Omega = 0$ in the GP equation (1). Fig. 1(a) shows the condensate density profile in the lattice potential without rotation. We then dynamically evolve Eq. (1) with a fixed angular velocigy Ω and look for equilibrium states. In addition to the condensate density profile, we also look at the density structure factor defined by

$$S(\mathbf{k}) = \int d\mathbf{r} n(\mathbf{r}) e^{-i\mathbf{k}\cdot\mathbf{r}}, \qquad (3)$$

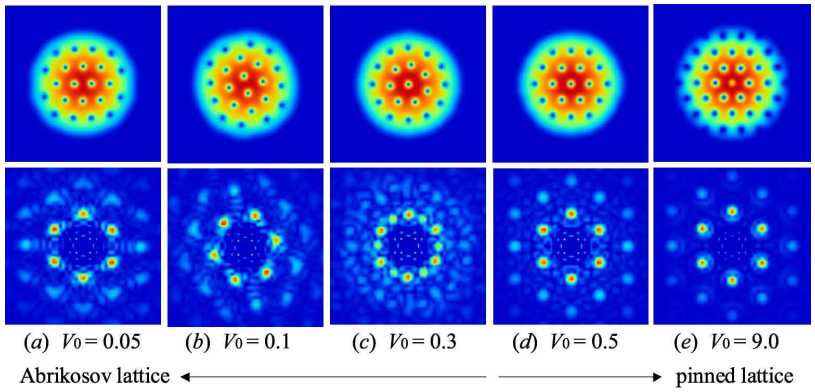

Fig. 2. Density profiles (upper) and Structure factor profiles (lower) of rotating condensates at $a/a_{ho} = 2.2$, $\sigma/a_{ho} = 0.65$ and $\Omega/\omega_0 = 0.70$. The figure show the vortex lattice structures corresponding to the intensity of the lattice potential : (a) $V_0 = 0.05$, (b) $V_0 = 0.1$, (c) $V_0 = 0.3$, (d) $V_0 = 0.5$, (e) $V_0 = 9.0$.

where $n(\mathbf{r}) = |\psi(\mathbf{r})|^2$ is condensate density. The structure factor provides us information about the periodicity of the condensate density. For triangular lattice geometry, there are periodic peaks of regular hexagonal geometry. By looking at the position of peaks of the structure factor, we can distinguish between the Abrikosov lattice and the pinned vortex lattice.

Fixing the lattice constant with $a/a_{ho} = 2.2$, we investigated the transition of the vortex lattice structure by changing the intensity V_0 for various angular velocities Ω/ω_0. Fig. 2 shows the density profiles and the structure factors for $\Omega/\omega_0 = 0.70$. One can see that for weak lattice potentials ((a) $V_0 = 0.05$, (b) $V_0 = 0.1$), vortices form the Abrikosov lattice, which is incommensurate with the lattice potential. By slightly increasing the intensity ((c) $V_0 = 0.3$), vortices start to being partially pinned by the lattice potentail. For strong lattice potentials ((d) $V_0 = 0.5$, (e) $V_0 = 9.0$), all vortices are pinned by the lattice potential. We thus observed the transition of the vortex lattice structure from the Abrikosov lattice to the pinned lattice.

In order to quantify the structural phase transition of the vortex lattice structure, we calculate the peak intensity of the structure factor $S(\mathbf{K})$ at the lattice pinning point, where $\mathbf{K}_1 = 2\pi/a(1, 1/\sqrt{3})$, $\mathbf{K}_2 = 2\pi/a(0, 2/\sqrt{3})$. In addition, we also calculate the lattice potential energy

$$E_{\text{lattice}} = \int d\mathbf{r}\psi^*(\mathbf{r})V_{\text{lattice}}(\mathbf{r})\psi(\mathbf{r}). \tag{4}$$

In Fig. 3, we plot $S(\mathbf{K})$ and E_{lattice} against of the intensity V_0. In Fig. 3(a) for $\Omega/\omega_0 = 0.70$, we find that E_{lattice} decreases gradually with vortices be-

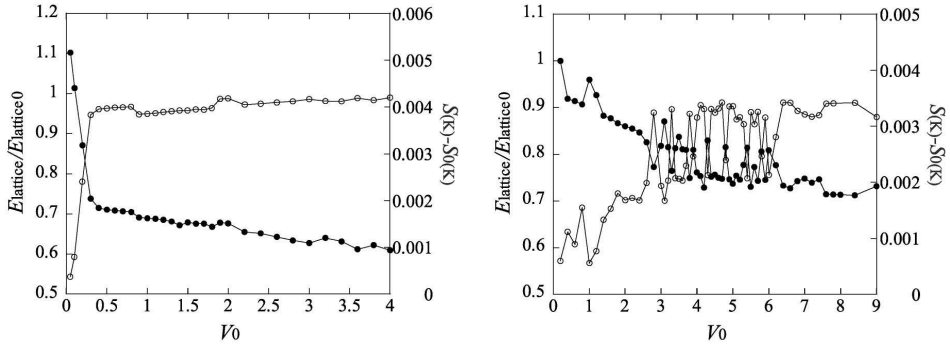

Fig. 3. Lattice potential energy (•) and peak intensity of the structure factor at the lattice pinning point (○) with $a/a_{ho} = 2.2$, $\sigma/a_{ho} = 0.65$ corresponding to the angular velocity: (*a*) $\Omega/\omega_0 = 0.70$, (*b*) $\Omega/\omega_0 = 0.55$. Here $E_{\rm lattice0}$ and $S_0(\mathbf{K})$ is the lattice energy and the peak intensity of the structure factor at the lattice pinning point of ground state for the intensity respectivity.

ing partially pinned, and reaches constant when all vortices are pinned for $V_0 > 0.4$. Correspondingly $S(\mathbf{K})$ increases gradually and finally becomes constant when all vortices are pinned. From these results together with directly looking at the condensate density profile, we conclude that the structural phase transition occurs at $V_0 = 0.4$. Fig. 3(b) shows the results for $\Omega/\omega_0 = 0.55$. In this case, there is an intermediate domain where the Abrikosov lattice and the pinnd lattice coexist. In this domain, the vortex lattice structure cannot be categorically determined because of the competition between the vortex-vortex interaction and the lattice pinning effect.

In Fig. 4, we map out the phase diagrams of the vortex lattice structures against Ω/ω_0 and V_0. The lower domain is the Abrikosov lattice domain, while the upper domain is the pinned lattice domain. The intermediate domain represents coexisting state of the Abrikosov lattice and the pinnd lattice. From Fig. 4(a) for $a/a_{ho} = 2.2$, we find that the pinning intensity takes the minimum value $V_{\rm min} = 0.4$ at $\Omega/\omega_0 = 0.70$. Similarly, we find $V_{\rm min} = 0.7$ at $\Omega/\omega_0 = 0.83$ for $a/a_{ho} = 2.0$ (as shown in Fig. 4(b)), and $V_{\rm min} = 1.0$ at $\Omega/\omega_0 = 0.65$ for $a/a_{ho} = 2.4$ (as shown in Fig. 4(c)).

The minimum values of the pinning lattice intensity V_0 for each lattice constant can be understood as follows. When vortices form the trianglular lattice and undergo rigid rotation with angular velocity Ω, the lattice

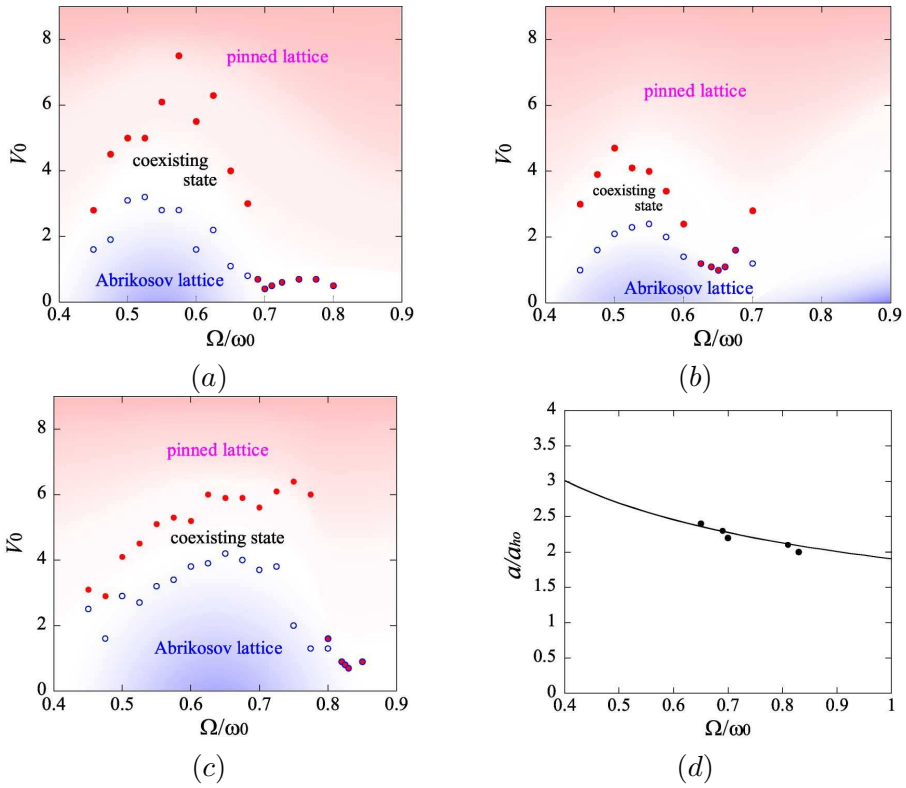

Fig. 4. (1) Phase diagrams for the vortex lattice structures: (a) $a/a_{ho} = 2.2$, (b) $a/a_{ho} = 2.4$, (c) $a/a_{ho} = 2.0$. (2) The angular verocity corresponding the minimum pinning intensity: (d). The solid line represents Eq. (5).

constant is expressed as a function of angular velocity by

$$a_v(\Omega)/a_{ho} = \sqrt{\frac{2}{\sqrt{3}}\frac{\kappa}{2\Omega/\omega_0}}, \tag{5}$$

where $\kappa = h/m$ is the circulation of a singly-quantized vortex. In Fig. 4(d), we plot the lattice constant a/a_{ho} against Ω/ω_0 giving the minimum pinning intensity. We find that it is well fitted by the funcion in Eq. (5). This means that the pinning intensity V_0 takes minimum value when $a_v(\Omega)$ matches to the lattice constant a. When this "matching relation" is satisfied, weak lattice potential has a stronger pinning effect than vortex-vortex interaction, which leads to a sharp transition of the vortex lattice structure.

In summary, we have studied the transition of the vortex lattice structures of Bose-Einstein condensates in a rotating triangular lattice potential. We showned that the transition is determined depending on parameters of the lattice potential. We also found that the lattice potential has a strong

pinning effect when the matching relation is satisfied. For a future study, we will discuss the transition of vortex lattice structures for various lattice potential geometries.

We thank S. Konabe and S. Watabe for useful discussions and comments. We also thank N. Sasa for helpful comments on the numerical simulations.

REFERENCES

1. K.W. Madison, F. Chevy, W. Wohlleben, and J. Dalibard, *Phys.Rev.Lett* **84**, 806 (2000).
2. K.W. Madison, F. Chevy, V. Bretin, and J. Dalibard, *Phys.Rev.Lett* **86**, 4443 (2001).
3. C. Raman, J.R. Abo-Shaeer, J.M. Vogels, K. Xu, and W. Ketterle, *Phys.Rev.Lett* **87**, 210402 (2001).
4. David L. Feder and Charles W. Clark, *Phys.Rev.Lett* **87**, 190401 (2001).
5. M. Tsubota, K. Kasamatsu, and M. Ueda, *Phys.Rev.A* **65**, 023603 (2002)
6. K. Kasamatsu, M. Tsubota, and M. Ueda, *Phys.Rev.A* **67**, 033610 (2003)
7. K. Kasamatsu, M. Tsubota, and M. Ueda, *Phys.Rev.A* **66**, 053606 (2002)
8. N. Sasa, M. Machida, and H. Matsumoto, *J. Low Temp. Phys* **138**, 617 (2005)
9. K. Kasamatsu, M. Machida, N. Sasa, and M. Tsubota, *Phys.Rev.A* **71**, 063616 (2005)
10. Alexander L. Fetter, B. Jackson, and S. Stringari, *Phys.Rev.A* **71**, 013605 (2005)
11. T. P. Simula, A.A. Penckwitt, and R.J. Ballagh, *Phys.Rev.Lett* **92**, 060401 (2004)
12. Rajiv Bhat, M.J. Holland, and L.D. Carr, *Phys.Rev.Lett* **96**, 060405 (2006)
13. J.W. Reijnders and R.A. Duine, *Phys.Rev.Lett* **93**, 060401 (2004).
14. H. Pu, L.O. Baksmaty, S. Yi, and N.P. Bigelow, *Phys.Rev.Lett* **94**, 190401 (2005).
15. S. Choi, S.A. Morgan, and K. Burnett, *Phys.Rev.A* **57**, 4057 (1998)
16. M.-O. Mewes, M.R. Andrews, N.J. van Druten, D.M. Kurn, D.S. Durfee, C.G. Townsend, and W. Ketterle, *Phys.Rev.Lett* **77**, 988 (1996)
17. B. Jackson and E. Zaremba, *Phys.Rev.Lett* **88**, 180402 (2002)
18. E. Zaremba, T. Nikuni, and A. Griffin, *J. Low Temp. Phys* **116**, 277 (1999)
19. D.S. Jin, M.R. Matthows, J.R. Ensher, C.E. Wieman, and E.A. Cornell, *Phys.Rev.Lett* **78**, 764 (1997).